# Seismic azimuthal anisotropy beneath the eastern United States and its geodynamic implications

**Bin B. Yang[1], Yunhua Liu[1,2] (iD), Haider Dahm[1,3] (iD), Kelly H. Liu[1] (iD), and Stephen S. Gao[1] (iD)**

[1]Geology and Geophysics Program, Missouri University of Science and Technology, Rolla, Missouri, USA, [2]CNPC Logging Co., Ltd, Xi'an, China, [3]Department of Geography, University of Misan, Amarah, Iraq

**Abstract** Systematic spatial variations of anisotropic characteristics are revealed beneath the eastern U.S. using seismic data recorded between 1988 and 2016 by 785 stations. The resulting fast polarization orientations of the 5613 measurements are generally subparallel to the absolute plate motion (APM) and are inconsistent with the strike of major tectonic features. This inconsistency, together with the results of depth estimation using the spatial coherency of the splitting parameters, suggests a mostly asthenospheric origin of the observed azimuthal anisotropy. The observations can be explained by a combined effect of APM-induced mantle fabric and a flow system deflected horizontally around the edges of the keel of the North American continent. Beneath the southern and northeastern portions of the study area, the E-W keel-deflected flow enhances APM-induced fabric and produces mostly E-W fast orientations with large splitting times, while beneath the southeastern U.S., anisotropy from the N-S oriented flow is weakened by the APM.

## 1. Introduction

As a nearly ubiquitous characteristic of the Earth's upper mantle, the azimuthal dependence of seismic velocities, i.e., azimuthal anisotropy, has been investigated for decades by numerous studies, mostly using shear wave splitting (SWS) analyses [e.g., *Francis*, 1969; *Leven et al.*, 1981; *Mainprice and Nicolas*, 1989; *Silver and Chan*, 1991; *Gao et al.*, 1994; *Savage*, 1999; *Yang et al.*, 2014, 2016]. In particular, splitting of $P$-to-$S$ converted phases (*SKS*, *SKKS*, and *PKS*, hereafter collectively called *XKS*) from the core-mantle boundary is among the most frequently employed structural seismological techniques to determine mantle anisotropy beneath the stations. Two parameters, including the fast orientation ($\phi$, which is the polarization orientation of the fast wave) and the splitting time ($\delta t$, which is the time difference between the fast and slow waves), are measured to quantify the anisotropy orientation and strength, respectively. The resulting measurements have an excellent lateral but limited vertical resolution [*Silver and Chan*, 1991; *Savage*, 1999; *Liu and Gao*, 2013], although under some ideal conditions, the depth of the source of anisotropy can be estimated with reasonable confidence using the spatial coherency of the splitting parameters [*Gao and Liu*, 2012].

Laboratory experiments and geodynamic modeling studies indicate that lattice preferred orientation (LPO) of the crystallographic axes of olivine is the most likely cause of mantle anisotropy [*Zhang and Karato*, 1995; *Becker et al.*, 2006]. The geodynamic implications of SWS observations are complicated by the fact that there is more than one mantle process that can lead to the LPO. For continental areas such as the eastern United States (EUS) that are away from active plate boundaries, the most likely processes include (1) simple shear originated from vertical flow gradient in the asthenosphere which leads to an anisotropy parallel to the flow direction, (2) lithospheric compression resulting in fast orientations consistent with the strike of the mountain belts [*Silver*, 1996, 1999; *Fouch and Rondenay*, 2006; *Long and Silver*, 2009; *Refayee et al.*, 2014], and (3) magmatic diking in the lithosphere that can lead to an observable dike-parallel seismic anisotropy [*Gao et al.*, 1997, 2008, 2010; *Walker et al.*, 2004; *Kendall et al.*, 2005]. Therefore, elucidating anisotropy-forming mechanisms for a given area is essential not only for understanding the origin of seismic anisotropy but also for characterizing past or current deformational processes in the mantle especially the existence and direction of mantle flow systems. The diverse tectonic features in the EUS and the recently recorded high-quality broadband seismic data make this area an ideal locale for in-depth investigations of seismic azimuthal anisotropy.
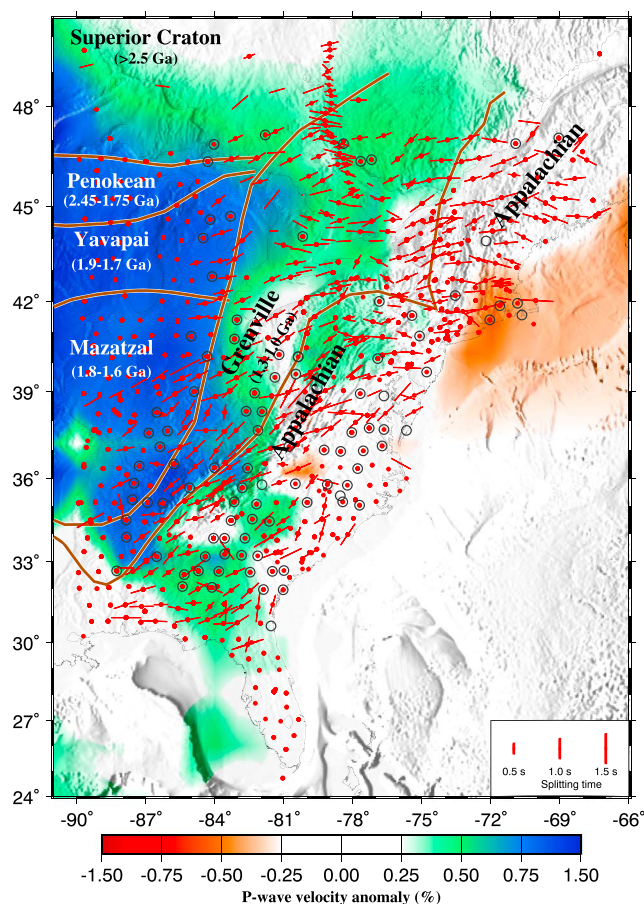
**Figure 1.** Map of the study area showing mean *P* wave velocity anomalies for the depth range of 100–200 km [*Burdick et al.*, 2014], major tectonic boundaries (brown lines), seismic stations (red dots) with one or more nonnull measurements from this study, and station-averaged shear wave splitting measurements (red bars) from previous studies [*Barruol et al.*, 1997; *Fouch et al.*, 2000; *Rondenay et al.*, 2000; *Eaton et al.*, 2004; *Frederiksen et al.*, 2006; *Long et al.*, 2010; *Wagner et al.*, 2012; *Long et al.*, 2016]. The orientation of the bars represents the fast orientation, and the length of the bars indicates the splitting time. Black circles show stations at which only null *SKS* splitting measurements were detected by *Long et al.* [2016], suggesting the absence of significant azimuthal anisotropy beneath the stations.

## 1.1. Tectonic Setting

The EUS, which is defined here as the land area of 67°W to 90°W and 24°N to 50°N (Figure 1), has experienced extension and compression of continental margins involving successive terrane accretions, orogenies, and continent breakup [*Thomas*, 2006; *Whitmeyer and Karlstrom*, 2007]. Main tectonic provinces include the Yavapai (1.9–1.7 Ga), Mazatzal (1.8–1.6 Ga), Grenville (1.3–1.0 Ga), and the Appalachian (0.26 Ga) [*Karlstrom and Bowring*, 1988; *Whitmeyer and Karlstrom*, 2007] (Figure 1). The Yavapai and Mazatzal provinces were related to accretion of juvenile volcanic arcs to the cratonic core [*Hoffman*, 1988], while the Grenville and Appalachian provinces were associated with the construction and breakup of Rodinia and Pangea [*Thomas*, 2006; *Whitmeyer and Karlstrom*, 2007; *Yuan et al.*, 2014].

Seismic tomographic studies suggest that the thickness of the lithosphere beneath the stable part of the North American Craton is 220–250 km and thins eastward to about 100–200 km at the Appalachian front [e.g., *van der Lee et al.*, 2008; *Yuan and Romanowicz*, 2010]. Mostly due to the eastward thinning of the lithosphere, the average upper mantle *P* wave velocities relative to the 1-D AK135 reference model reduce systematically toward the edges of the continent (Figure 1) [*Burdick et al.*, 2014].

## 1.2. Previous Shear Wave Splitting Studies in the EUS

Numerous SWS studies in the EUS have been conducted since the early 1990s (Figure 1) [e.g., *Vinnik et al.*, 1992; *Barruol et al.*, 1997; *Fouch et al.*, 2000; *Frederiksen et al.*, 2007; *Long et al.*, 2016], with significantly different results at the same or nearby stations and different proposed mechanisms for the origin of the observed

seismic anisotropy. *Barruol et al.* [1997] reported mostly E-W fast orientations with larger than global averaged splitting times of 1.0 s along the transition zone between the northern and central sections of the EUS. They proposed that the local dominance of E-W mantle flow or/and fossil lithospheric deformation contributed to the observed seismic anisotropy. Null splitting observations indicating the absence of significant azimuthal anisotropy were found at two stations near the coast and were attributed to rifting-induced magmatic intrusion that would serve to weaken preexisting lithospheric fabric. A more recent study [*Fouch et al.*, 2000] proposed that the bulk of the observed anisotropy in eastern North America can be satisfactorily explained by mantle flow around the keel of the continent. Keel-modified mantle flow was also proposed by *Eaton et al.* [2004] based on SWS measurements at 24 stations.

Using Pre-USArray data, *Long et al.* [2010] and *Wagner et al.* [2012] showed a contrast in splitting behavior between stations located in the Appalachian province and those located closer to the eastern coast, where they observed null *SKS* splitting parameters indicating that beneath most of the stations, the crust and mantle are overall azimuthally isotropic. They proposed that the difference in splitting patterns is consistent with a transition from drag-induced asthenospheric flow beneath the North American Craton to vertical or incoherent mantle flow. The most recent SWS study in the EUS [*Long et al.*, 2016] used data recorded by the USArray Transportable Array (TA) stations prior to August 2014, when most of the TA stations were still recording in the eastern part of the study area. Similar to *Long et al.* [2010] and *Wagner et al.* [2012], *Long et al.* [2016] found that the southeastern U.S. is dominated by stations with null *SKS* measurements (shown as black circles in Figure 1) that are attributable to either vertical flow or vertically incoherent lithospheric anisotropy.

As shown below, the combination of the fact that only the *SKS* phase (rather than *PKS*, *SKKS*, and *SKS*) was used and the short recording time at some of the stations might have resulted in limited azimuthal coverage of the events used in previous SWS studies, preventing reliable identification of detectable azimuthal anisotropy and leading to the conclusion of widespread existence of mantle azimuthal isotropy (Figure 1). In addition, SWS measurements have not been obtained at about 100 stations in the EUS (Figure 1). This study represents the final phase of a long-lasting effort to produce a uniform SWS database for the contiguous U.S. using data recorded by both permanent and campaign-style (including the USArray TA) stations, for the ultimate goal of providing critical constraints on the structural and geodynamic models of the Earth's mantle beneath the North American plate [*Liu*, 2009; *Liu et al.*, 2014; *Yang et al.*, 2016].

## 2. Data and Methods

Data used in this study were recorded by 785 broadband seismic stations (red dots in Figure 1) located in the area of 24–50°N and 90–67°W archived at the Incorporated Research Institutions for Seismology (IRIS) Data Management Center (DMC), including 497 stations from the TA and 288 from other networks. Seismograms were recorded during a maximum period of about 28 years from late 1988 to May 2016, at which moment all the USArray TA stations had finished recording in the EUS.

The detailed procedure for measuring and ranking the splitting parameters is described in *Liu* [2009] and *Liu and Gao* [2013] and is briefly summarized below. The procedure is based on the minimization of transverse energy technique [*Silver and Chan*, 1991]. Seismograms are extracted from events with a cutoff magnitude of 5.6, which is reduced to 5.5 for earthquakes with focal depths deeper than 100 km. To ensure that all the usable XKS signals are included in the study, the epicentral distance range for *PKS*, *SKKS*, and *SKS* used for data requesting is 120–180°, 95–180°, and 84–180°, respectively [*Liu and Gao*, 2013], although the vast majority of the events have an epicentral distance in the range of 90–130° (Figure 2a, inset). An initial band-pass filter with corner frequencies of 0.04 and 0.5 Hz is applied to all the seismograms.

The final stage of the procedure is to manually verify the results and adjust (if necessary) the measuring parameters, including the beginning and end of the XKS window and the band-pass filtering frequencies, for each of the measurements by visually checking the quality of the original and corrected radial and transverse components, the waveform fit between the resulting fast and slow components, the linearity of the corrected particle motions, and the significance and uniqueness of the minimum value point on the contour map of the energy of the corrected transverse component (Figure S1 in the supporting information). The resulting SWS measurements are grouped into Quality A (outstanding), B (good), C (unusable), and N (null: strong XKS energy on the radial but no observable XKS energy on the transverse component) quantitatively based on the signal-to-noise ratio on the original and corrected radial and transverse components and the uniqueness of the minimum energy peaks [*Liu et al.*, 2008].
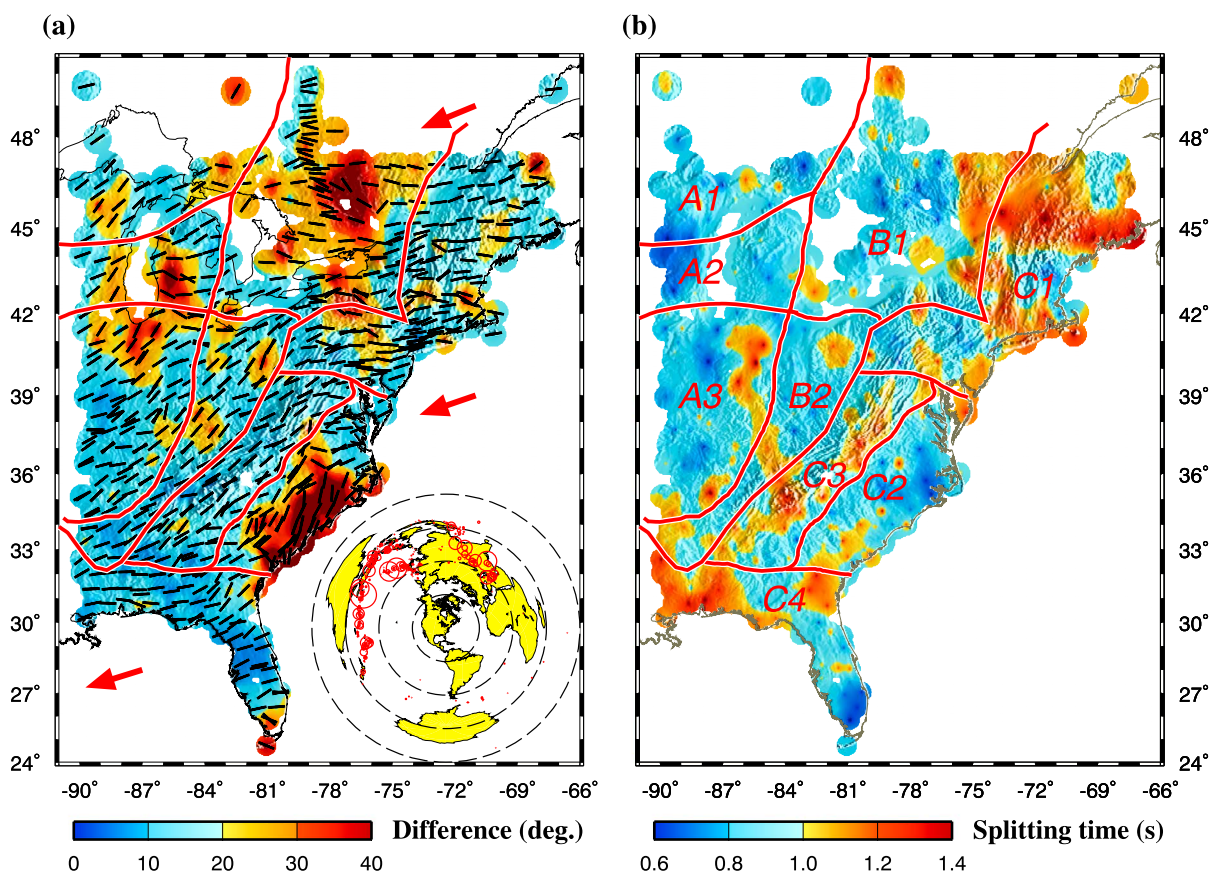
**Figure 2.** (a) Station-averaged (black bars) fast orientations from this study plotted at the stations. The background image shows the absolute difference between the fast orientation and the APM direction computed at each of the stations. Red arrows show the APM direction [*Gripp and Gordon*, 2002], and the red lines divide the area into nine regions. The 556 earthquakes used in the study are shown as red circles (whose size is proportional to the number of Quality A or B measurements that the event produces) in the inset azimuthal equidistant projection map, in which the concentric circles indicate the epicentral distance from the center of the study area with an increment of 45°. (b) Spatial distribution of the resulting splitting times.

## 3. Results

A total of 5613 pairs of nonnull SWS measurements is obtained at 785 stations, including 1187 from *PKS*, 928 from *SKKS*, and 3498 from *SKS* (Table S1 and Figure S2). The total number of nonnull measurements produced by this study is about 10 times that reported by the most recent SWS study for the EUS [*Long et al.*, 2016], which used only the *SKS* phase from the TA stations recorded prior to August 2014. Another possible reason for the difference in the number of nonnull measurements (and the pervasive null-stations reported in the latter) might be related to the different band-pass filtering frequency ranges, which is 0.04–0.5 Hz for this and 0.02–0.125 Hz for the other study. The low frequencies make it difficult to detect splitting with a $\delta t$ of 0.5 s or smaller [*Long et al.*, 2016]. The simple mean of the splitting times is 0.98 ± 0.31 s which is equivalent to the global average of 1.0 s for continents [*Silver*, 1996], while the circular mean for the fast orientations is 67.5 ± 24.3° (or 247.5° measured clockwise from the north) which is almost identical to the absolute plate motion (APM) direction of 246–253° for the EUS in the fixed hot spot model [*Gripp and Gordon*, 2002]. The station-averaged measurements are shown in Figure 2, and the individual and station-averaged splitting parameters can be found in the supporting information as Tables S1 and S2, respectively. (Note that waveform and other related plots similar to those shown in Figure S1 for all the 5613 measurements can be found at http://www.mst.edu/%7Esgao/YangEUS, which will be merged with the IRIS DMC Data Product that we produced for the western and central U.S.: http://ds.iris.edu/ds/products/sws-db-mst/).

We visually check the resulting splitting parameters for each of the stations to search for systematic azimuthal variations to identify potential existence of significant complex anisotropy [*Silver and Savage*, 1994] and conclude that a one-layer anisotropy model with a horizontal axis of symmetry is sufficient to explain the vast majority of the observed splitting parameters. This conclusion, however, does not exclude multiple layer

models with parallel or perpendicular fast orientations. In addition, due to the fact that all the stations with reliable XKS arrivals on the radial component have one or more nonnull XKS splitting measurements, null measurements are not reported because they simply reflect the fact that the back azimuth of the events and the fast orientation are nearly parallel or orthogonal to each other [*Silver and Chan*, 1991; *Liu and Gao*, 2013]. To facilitate data presentation and interpretation, in the following we divided the study area into nine regions (Figure 2b), based on the tectonic setting and the characteristics of the splitting parameters

### 3.1. Regions A1–A3
Regions A1–A3 are situated on the Early Proterozoic basement west of the Grenville Front. Only a small fraction of the stations have previously reported SWS measurements, and *Long et al.* [2016] observed a set of null-dominated stations in Regions A2 and A3 (Figure 1). The mean splitting times for the three regions are 0.91–0.95 s, which are smaller than the global average of 1.0 s and are consistent with those observed on the western part of the stable North American continent using the same procedure [*Yang et al.*, 2016]. While the majority of the fast orientations are within 20° from the APM, larger deviations are found in the Great Lakes area. The fast orientations observed in the eastern part of A1 and A2 as well as those in the NE corner of A3 are mostly E-W, which is also the dominant orientation for the other northern regions (B1 and C1). Most of the fast orientations are at a large angle with the strike of the major terrane boundaries (Figure 2a).

### 3.2. Regions B1 and B2
Regions B1 and B2 are in the Mid-Proterozoic Grenville Province. The fast orientations in B1 are mostly E-W or NW-SE, and those in B2 are mostly parallel to the APM direction. The transition from mostly E-W fast orientations to NE-SW ones takes place gradually along the boundary between B1 and B2, over a distance of about 200 km. Large splitting times are found in the NE corner of Region B1.

### 3.3. Regions C1–C4
Regions C1–C4 belong to the Appalachian province. The fast orientations in C1 are almost consistently E-W, which is approximately in agreement with the APM but nearly 45° from the dominantly NE-SW strike of the Appalachians. This region has the largest splitting times in the entire study area.

Splitting parameters observed in Region C2 are anomalous in terms of the dominantly N-S fast orientations that are not observed in other regions and the small splitting times which might be partially responsible for the widespread null measurements reported by previous studies [e.g., *Long et al.*, 2010; *Wagner et al.*, 2012; *Long et al.*, 2016].

Region C3 is the southernmost part of the Appalachians. The splitting times are comparable to the global average, and the fast orientations are subparallel to both the APM and the main strike of the Appalachians. One interesting observation is that while the strike of the Appalachians changes by about 30° at about 37–38°N latitude, no corresponding changes are found in the observed fast orientations.

The resulting fast orientations in the western part of Region C4 are mostly E-W. The large splitting times and the E-W fast orientations are consistent with those observed along the Texas coastline [*Refayee et al.*, 2014]. The fast orientations make a gradual NE-SW turn in the eastern part of this region.

## 4. Discussion
### 4.1. Depth of the Anisotropic Layer
The numerous spatially varying splitting parameters observed at densely spaced stations make the study area an ideal locale to apply the spatial coherency approach [*Gao et al.*, 2010; *Liu and Gao*, 2011] for estimating the depth of the center (weighted by the degree of anisotropy if it is unevenly distributed vertically) of the anisotropic layer for each of the nine regions. The resulting optimal depth corresponding to the minimum variation factor ranges from about 140 km beneath Region C1 to 240 km beneath A1 (Figure 3). On average, there is an eastward shallowing of the estimated depths, which is consistent with the eastward decrease of seismic *P* wave velocities [*Burdick et al.*, 2014] (Figure 3c). The resulting depth estimates, when compared with the thickness of the lithosphere proposed by previous seismic tomographic studies [*van der Lee*, 2002; *Li et al.*, 2003; *Yuan and Romanowicz*, 2010], suggest that the observed anisotropy is mostly from the upper asthenosphere. This conclusion of mainly asthenospheric origin is consistent with that obtained in the central U.S. based on the same spatial coherency procedure [*Refayee et al.*, 2014; *Yang et al.*, 2014].

While contributions from lithospheric fabric to the observed anisotropy cannot be completely ruled out, the following observations imply that lithospheric contributions to the observed azimuthal anisotropy are
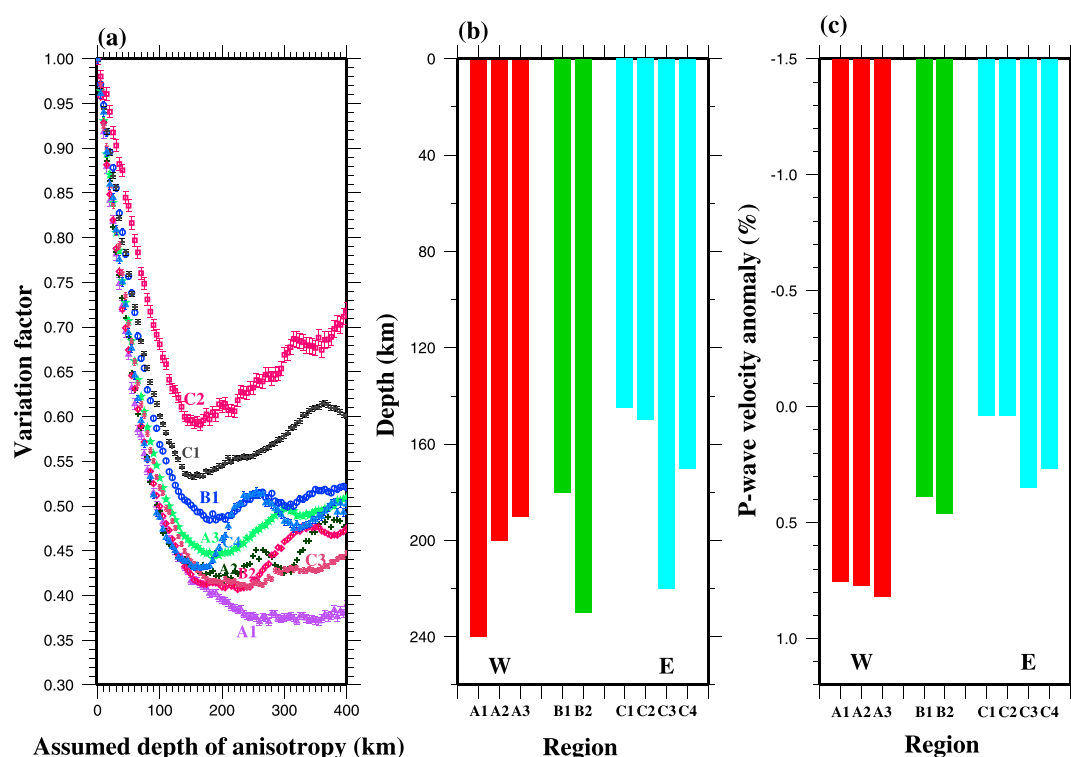
**Figure 3.** Anisotropy depth analysis for the nine regions using a bin size of 0.2° [*Gao and Liu*, 2012]. (a) Curves of the variation factors. (b) The resulting depth for each region. (c) The upper mantle mean velocity anomaly relative to the AK135 model for each of the nine regions [*Burdick et al.*, 2014].

insignificant: (1) there is a large angular difference between the fast orientations and the dominant strike of most of the major tectonic boundaries and features in many of the areas (Figures 1 and 2a), (2) the largest splitting times are observed in areas with thin lithosphere in the study area (e.g., C1 and C4), (3) there is no significant increase in the splitting times along major terrane boundaries (Figure 2b, in which most of the area boundaries are the same as the tectonic terrane boundaries shown in Figure 1). Such an increase is expected if the degree of anisotropy positively correlates to compressional strain, and (4) the estimated depth of the center of the anisotropic layer discussed above is greater than the tomographically derived thickness of the lithosphere.

If the observed anisotropy is a combination of deformation in the asthenosphere and lithosphere, as proposed by some of the previous studies, a two-layer anisotropic structure is present, which produces azimuthally varying splitting parameters with a 90° periodicity (with the exception of the situation that the fast orientations of the two layers are consistently parallel or orthogonal to each other). Such an azimuthal variation is not observed, and thus, the SWS observations are mostly from a single layer of anisotropy (or multiple layers with approximately parallel or orthogonal fast orientations) in the upper asthenosphere.

### 4.2. Keel-Deflected Mantle Flow and APM-Induced Anisotropy

Some of the most recent seismic tomographic studies [e.g., *Burdick et al.*, 2014] suggest that a large portion of the eastern margin of the North American cratonic keel, which tilts toward the continental interior on the vertical plane, is not parallel to the NE-SW strike of the coastline but instead is mostly N-S oriented (Figure 1). On the horizontal plane, the strike of the keel makes a sharp turn in the northern part of the study area and becomes mostly E-W, as exemplified by one of the recent tomographic images (Figure 1) [*Burdick et al.*, 2014]. The SWS observations can be well explained by a simple model involving both APM-induced fabric and a mantle flow system deflected horizontally around the lateral edges of the keel of the North American Craton [*Fouch et al.*, 2000; *Refayee et al.*, 2014; *Yang et al.*, 2014]. We propose that the APM-induced flow system ($V_c$) is mainly developed in the transitional layer between the partially coupled lithosphere and the asthenosphere and is present beneath the entire area, while the horizontally deflected flow system exists only beneath the cratonic edges and goes around the keel (Figure 4). Note that both flow systems are relative to the solid
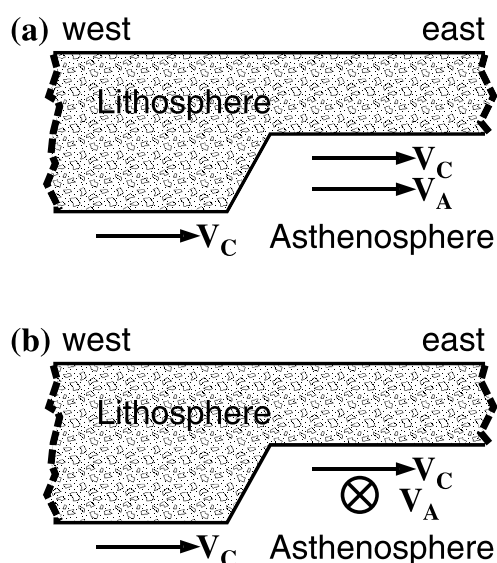
**Figure 4.** Schematic diagrams showing possible flow fields (relative to the lithosphere) responsible for the generation of the observed anisotropy. (a) An E-W vertical section across the entire northern or southern portion of the study area with dominantly E-W fast orientations and larger-than-normal splitting times. $V_C$ represents simple shear in the transitional layer between the partially coupled lithosphere and asthenosphere, and $V_A$ is a system of asthenospheric flow traveling horizontally around the edges of the cratonic keel beneath the transitional layer. (b) Same as Figure 4a but for a profile traversing the area with mostly N-S fast orientations and reduced splitting times in the SE U.S. Note that similar anisotropic characteristics can be obtained if all the flow vectors reverse their direction.

lithosphere. Studies suggest that the lithosphere-asthenosphere boundary (LAB) beneath the portion of the study area with thick cratonic mantle lithosphere is represented by a gradual change over a vertical distance of 70 or more kilometers, and that the LAB beneath thinner lithosphere could be as gradual as 30–40 km [*Abt et al.*, 2010; *Fischer et al.*, 2010]. Simple shear in this transitional layer of the two rheologically different zones can produce significant anisotropy [*McKenzie*, 1979; *Conrad and Behn*, 2010]; for instance, a layer of 100 km with an average anisotropy of 4% can produce the observed splitting times of 1 s. The keel-deflected flow system, on the other hand, is most likely in the low viscous asthenosphere beneath the transitional layer (Figure 4).

This model attributes the dominantly APM-parallel fast orientations observed in the cratonic interior to the simple shear induced by the relative motion between the lithosphere and asthenosphere along the APM direction. In contrast, the nearly E-W fast orientations and the large splitting times observed along the southern and NE portions of the study area are due to a combined effect of keel-deflected mantle flow and APM-induced fabric, which are approximately consistent with each other (with an ~20° or less difference; Figure 4a). Finally, the model attributes the mostly N-S fast orientations and the small splitting times observed in the southeastern U.S. (Region C2) to the canceling effect of the approximately N-S oriented keel-deflected flow and the E-W oriented APM-induced anisotropies

(Figure 4b). It has long been recognized that in a two-layered system of anisotropy of orthogonal fast orientations, the combined fast orientation of the system is that of the layer with the larger splitting time, and the combined splitting time is the difference between the splitting times of the two layers [*Silver and Savage*, 1994]. Therefore, the fact that the resulting fast orientations are mostly N-S suggests that anisotropy from keel-deflected flow is stronger than that associated with APM-related fabric.

It must be pointed out that results from SWS analyses alone cannot unambiguously reveal the directions (relative to the lithosphere) of the flow systems. For instance, a westward moving plate on top of a stationary or eastward moving asthenosphere plus a mostly eastward deflected flow system (except for the SE U.S. where it moves northward) can produce the main characteristics of the observed anisotropy (Figure 4), as discussed above. Similarly, a westward moving flow system beneath the plate together with a mostly westward deflected flow system (except for the SE U.S. where it moves southward) can also produce the observed pattern of anisotropy. The key to distinguish these models of plate dynamics is to conduct geodynamic modeling by taking into account of the true geometry of the LAB and accurately determined velocity and density models, and by using other geophysical observations such as shear wave splitting measurements as constraints.

## 5. Conclusions

By utilizing all the available broadband seismic data recorded in the EUS prior to May 2016 including those from the USArray TA stations, we have revealed systematic spatial variations of seismic azimuthal anisotropy at 785 stations. The observations can best be explained by the combined effects of two anisotropy-forming mechanisms, including APM-parallel simple shear developed in the transitional layer between the partially coupled lithosphere and asthenosphere, and an asthenospheric flow system around the southern and eastern

keels of the North American Craton. We propose that while the former is the dominating mechanism for the APM-parallel anisotropy observed in the cratonic interior, the combination of the two deformation systems creates the mostly E-W strong anisotropy along the southern and NE portions of the study area, as well as the N-S oriented weak anisotropy observed in the southeastern U.S.

## References

Abt, D. L., K. M. Fischer, S. W. French, H. A. Ford, H. Yuan, and B. Romanowicz (2010), North American lithospheric discontinuity structure imaged by *Ps* and *Sp* receiver functions, *J. Geophys. Res.*, *115*, B09301, doi:10.1029/2009JB006914.

Barruol, G., P. G. Silver, and A. Vauchez (1997), Seismic anisotropy in the eastern United States: Deep structure of complex continental plate, *J. Geophys. Res.*, *102*, 8329–8348.

Becker, T. W., S. Chevrot, V. Schulte-Pelkum, and D. K. Blackman (2006), Statistical properties of seismic anisotropy predicted by upper mantle geodynamic models, *J. Geophys. Res.*, *111*, B08309, doi:10.1029/2005JB004095.

Burdick, S., R. D. Van Der Hilst, F. L. Vernon, V. Martynov, T. Cox, J. Eakins, G. H. Karasu, J. Tylell, L. Astiz, and G. L. Pavlis (2014), Model update January 2013: Upper mantle heterogeneity beneath North America from travel-time tomography with global and USArray transportable array data, *Seismol. Res. Lett.*, *85*, 77–81, doi:10.1785/0220130098.

Conrad, C. P., and M. D. Behn (2010), Constraints on lithosphere net rotation and asthenospheric viscosity from global mantle flow models and seismic anisotropy, *Geochem. Geophys. Geosyst.*, *11*, Q05W05, doi:10.1029/2009GC002970.

Eaton, D. W., A. W. Frederiksen, and S. K. Miong (2004), Shear wave splitting observations in the lower Great Lakes region: Evidence for regional anisotropic domains and keel-modified asthenospheric flow, *Geophys. Res. Lett.*, *31*, L07610, doi:10.1029/2004GL019438.

Fischer, K. M., H. A. Ford, D. L. Abt, and C. A. Rychert (2010), The lithosphere-asthenosphere boundary, *Annu. Rev. Earth Planet. Sci.*, *38*, 551–575, doi:10.1146/annurev-earth-040809-152438.

Fouch, M. J., and S. Rondenay (2006), Seismic anisotropy beneath stable continental interiors, *Phys. Earth Planet. Inter.*, *158*, 292–320, doi:10.1016/j.pepi.2006.01.022.

Fouch, M. J., K. M. Fischer, E. M. Parmentier, M. E. Wysession, and T. J. Clarke (2000), Shear wave splitting, continental keels, and patterns of mantle flow, *J. Geophys. Res.*, *105*, 6255–6275.

Francis, T. J. G. (1969), Generation of seismic anisotropy in the upper mantle along the mid-ocean ridges, *Nature*, *221*, 162–165.

Frederiksen, A. W., I. J. Ferguson, D. Eaton, S.-K. Miong, and E. Gowan (2006), Mantle fabric at multiple scales across an Archean-Proterozoic boundary, Eastern Ontario, Canada, *Phys. Earth Planet. Inter.*, *158*, 240–263.

Frederiksen, A. W., S.-K. Miong, F. A. Darbyshire, D. W. Eaton, S. Rondenay, and S. Sol (2007), Lithospheric variations across the Superior Province, Ontario, Canada: Evidence from tomography and shear wave splitting, *J. Geophys. Res.*, *112*, B07318, doi:10.1029/2006JB004861.

Gao, S., P. M. Davis, H. Liu, P. D. Slack, Y. A. Zorin, V. V. Mordvinova, V. M. Kozhevnikov, and R. P. Meyer (1994), Seismic anisotropy and mantle flow beneath the Baikal rift zone, *Nature*, *371*, 149–151.

Gao, S. S., and K. H. Liu (2012), AnisDep: A FORTRAN program for the estimation of the depth of anisotropy using spatial coherency of shear-wave splitting parameters, *Comput. Geosci.*, *49*, 330–333.

Gao, S. S., P. M. Davis, K. H. Liu, P. D. Slack, A. W. Rigor, Y. A. Zorin, V. V. Mordvinova, V. M. Kozhevnikov, and N. A. Logatchev (1997), SKS splitting beneath continental rift zones, *J. Geophys. Res.*, *102*, 22,781–22,797.

Gao, S. S., K. H. Liu, R. J. Stern, G. R. Keller, J. P. Hogan, J. Pulliam, and E. Y. Anthony (2008), Characteristics of mantle fabrics beneath the south-central United States: Constraints from shear-wave splitting measurements, *Geosphere*, *4*, 411–417, doi:10.1130/GES00159.1.

Gao, S. S., K. H. Liu, and M. G. Abdelsalam (2010), Seismic anisotropy beneath the Afar Depression and adjacent areas: Implications for mantle flow, *J. Geophys. Res.*, *115*, B12330, doi:10.1029/2009JB007141.

Gripp, A. E., and R. G. Gordon (2002), Young tracks of hotspots and current plate velocities, *Geophys. J. Int.*, *150*, 321–361.

Hoffman, P. F. (1988), United plates of America, the birth of a craton: Early Proterozoic assembly and growth in Laurentia, *Annu. Rev. Earth Planet. Sci.*, *16*, 543–603.

Karlstrom, K. E., and S. A. Bowring (1988), Early Proterozoic assembly of tectono-stratigraphic terranes in southwestern North America, *J. Geol.*, *96*, 561–576.

Kendall, J.-M., G. W. Stuart, C. Ebinger, I. D. Bastow, and D. Keir (2005), Magma-assisted rifting in Ethiopia, *Nature*, *433*, 146–148.

Leven, J. N., L. Jackson, and A. E. Ringwood (1981), Upper mantle seismic anisotropy and lithospheric decoupling, *Nature*, *289*, 234–239.

Li, A., D. W. Forsyth, and K. M. Fischer (2003), Shear velocity structure and azimuthal anisotropy beneath eastern North America from Rayleigh wave inversion, *J. Geophys. Res.*, *108*(B8), 2362, doi:10.1029/2002JB002259.

Liu, K. H. (2009), NA-SWS-1.1: A uniform database of teleseismic shear-wave splitting measurements for North America, *Geochem. Geophys. Geosyst.*, *10*, Q05011, doi:10.1029/2009GC002440.

Liu, K. H., and S. S. Gao (2011), Estimation of the depth of anisotropy using spatial coherency of shear-wave splitting parameters, *Bull. Seismol. Soc. Am.*, *101*, 2153–2161.

Liu, K. H., and S. S. Gao (2013), Making reliable shear-wave splitting measurements, *Bull. Seismol. Soc. Am.*, *103*, 2680–2693, doi:10.1785/0120120355.

Liu, K. H., S. S. Gao, Y. Gao, and J. Wu (2008), Shear wave splitting and mantle flow associated with the deflected Pacific slab beneath northeast Asia, *J. Geophys. Res.*, *113*, B01305, doi:10.1029/2007JB005178.

Liu, K. H., A. Elsheikh, A. Lemnifi, U. Purevsuren, M. Ray, H. Refayee, B. B. Yang, Y. Yu, and S. S. Gao (2014), A uniform database of teleseismic shear wave splitting measurements for the western and central United States, *Geochem. Geophys. Geosyst.*, *15*, 2075–2085, doi:10.1002/2014GC005267.

Long, M. D., and P. G. Silver (2009), Shear wave splitting anisotropy: Measurements, interpretation, and new directions, *Survey Geophys.*, *30*, 407–461.

Long, M. D., M. H. Benoit, M. C. Chapman, and S. D. King (2010), Upper mantle anisotropy and transition zone thickness beneath southeastern North America and implications for mantle dynamics, *Geochem. Geophys. Geosyst.*, *11*, Q10012, doi:10.1029/2010GC003247.

Long, M. D., K. G. Jackson, and J. F. McNamara (2016), SKS splitting beneath Transportable Array stations in eastern North America and the signature of past lithospheric deformation, *Geochem. Geophys. Geosyst.*, *17*, 2–15, doi:10.1002/2015GC006088.

Mainprice, D., and A. Nicolas (1989), Development of shape and lattice preferred orientations: Application to the seismic anisotropy of the lower crust, *J. Struct. Geol.*, *11*, 175–189.

McKenzie, D. P. (1979), Finite deformation during fluid flow, *Geophys. J. R. Astron. Soc.*, *58*, 689–715.

Refayee, H. A., B. B. Yang, K. H. Liu, and S. S. Gao (2014), Mantle flow and lithosphere-asthenosphere coupling beneath the southwestern edge of the North American Craton: Constraints from shear-wave splitting measurements, *Earth Planet. Sci. Lett.*, *402*, 209–220, doi:10.1016/j.epsl.2013.01.031.

Rondenay, S., M. G. Bostock, T. M. Hearn, D. J. White, and R. M. Ellis (2000), Lithospheric assembly and modification of the SE Canadian Shield: Abitibi-Grenville Teleseismic Experiment, *J. Geophys. Res.*, *105*, 13,735–13,754.

Savage, M. K. (1999), Seismic anisotropy and mantle deformation: What we learned from shear-wave splitting?, *Rev. Geophys.*, *37*, 65–106.

Silver, P. G. (1996), Seismic anisotropy beneath the continents: Probing the depths of geology, *Annu. Rev. Earth Planet. Sci.*, *24*, 385–432.

Silver, P. G., and W. W. Chan (1991), Shear wave splitting and subcontinental mantle deformation, *J. Geophys. Res.*, *96*, 16,429–16,454.

Silver, P. G., and M. Savage (1994), The interpretation of shear-wave splitting parameters in the presence of two anisotropic layers, *Geophys. J. Int.*, *119*, 949–963.

Thomas, W. A. (2006), Tectonic inheritance at a continental margin, *GSA Today*, *16*, 4–11, doi:10.1130/1052-5173(2006)016.

van der Lee, S. (2002), High-resolution estimates of lithospheric thickness from Missouri to Massachusetts, USA, *Earth Planet. Sci. Lett.*, *203*, 15–23.

van der Lee, S., K. Regenauer-Lieb, and D. A. Yuen (2008), The role of water in connecting past and future episodes of subduction, *Earth Planet. Sci. Lett.*, *273*, 15–27, doi:10.1016/j.epsl.2008.04.041.

Vinnik, L. P., L. I. Makeyeva, A. Milev, and A. Y. Usenko (1992), Global patterns of azimuthal anisotropy and deformations in the continental mantle, *Geophys. J. Int.*, *111*, 433–447.

Wagner, L. S., M. D. Long, M. D. Johnston, and M. H. Benoit (2012), Lithospheric and asthenospheric contributions to shear-wave splitting observations in the southeastern United States, *Earth Planet. Sci. Lett.*, *341*, 128–138, doi:10.1016/j.epsl.2012.06.020.

Walker, K. T., A. A. Nyblade, S. L. Klemperer, G. H. R. Bokelmann, and T. J. Owens (2004), On the relationship between extension and anisotropy: Constraints from shear wave splitting across the East African Plateau, *J. Geophys. Res.*, *109*(B18), 8302, doi:10.1029/2003JB002866.

Whitmeyer, S. J., and K. E. Karlstrom (2007), Tectonic model for the Proterozoic growth of North America, *Geosphere*, *34*, 220–259.

Yang, B. B., S. S. Gao, K. H. Liu, A. A. Elsheikh, A. A. Lemnifi, H. A. Refayee, and Y. Yu (2014), Seismic anisotropy and mantle flow beneath the northern Great Plains of North America, *J. Geophys. Res. Solid Earth*, *119*, 1971–1985, doi:10.1002/2013JB010561.

Yang, B. B., K. H. Liu, H. H. Dahm, and S. S. Gao (2016), A uniform database of teleseismic shear wave splitting measurements for the western and central United States: December 2014 update, *Seismol. Res. Lett.*, *87*, 295–300, doi:10.1785/0220150213.

Yuan, H., and B. Romanowicz (2010), Lithospheric layering in the North American craton, *Nature*, *466*, 1063–1069.

Yuan, H., S. French, P. Cupillard, and B. Romanowicz (2014), Lithospheric expression of geological units in central and eastern North America from full waveform tomography, *Earth Planet. Sci. Lett.*, *402*, 176–186, doi:10.1016/j.epsl.2013.11.057.

Zhang, S., and S. I. Karato (1995), Lattice preferred orientation of olivine aggregates deformed in simple shear, *Nature*, *375*, 774–777.